Engineering Failure Analysis 75 (2017) 1–14

Contents lists available at ScienceDirect

Engineering Failure Analysis

journal homepage: www.elsevier.com/locate/engfailanal

Failure and integrity analysis of casings used for oil well drilling

Pablo. G. Cirimello [a], Jose L. Otegui [a,b,*], Guillermo Carfi [a], Walter Morris [a]

[a] YPF Tecnología S.A., Av. del Petróleo Arg. s/n, 1923 Berisso, Argentina
[b] Y-TEC, Conicet, Argentina

ARTICLE INFO

Article history:
Received 16 September 2016
Received in revised form 4 November 2016
Accepted 7 November 2016
Available online 10 November 2016

Keywords:
Casing drilling
Fatigue cracking
In-service integrity
Material optimization

ABSTRACT

Drilling with casing (DwC) is an innovative method particularly widespread in deep shale plays, that reduces the time and cost of drilling stages. However, casings are not designed for this purpose, and still the pipes and connections are required to remain sealed in the well after sustaining a large amount of drilling cycles and possible damage. The investigations presented in this article were triggered by the failure of a 9 5/8″ diameter K55 seamless casing during drilling an oil well. Fractographic analyses identified fatigue crack nucleation and growth in the tube/coupling (T/C) transition zone. The failure analysis included physical and chemical material tests and numerical stress analyses at the T/C threaded joints when subjected to the loads logged during drilling.

Fatigue cracks were found in other pipes that, although did not lead to fast fracture, would have caused leaking during subsequent well completion and production. The most relevant conclusion is that future integrity of casings used for drilling could not be assured. Reducing cyclic drilling stresses below the actual fatigue strength of pipes and connections is not easy task; the industry tendency is to go to slim-hole DwC, with ever increasing operating loads. Therefore, the economic feasibility of using heat treated casing and more sophisticated DwC designs are highlighted. Large grained tube steels and premium connections are found to be the most cost-effective alternatives to ensure the casing would survive the cyclic torque and compression stresses without serious damage.

1. Introduction

Drilling with Casing (DwC) is an innovative method particularly widespread in deep shale plays, that reduces the time and cost of drilling stages. Traditional drill pipes that transmit torque and compression to the drilling bit are replaced by the same tube that will later become the well casing [1].

The applicability of the concept of Drilling with Casing, also called Casing while Drilling (CwD) or simply Casing Drilling (C–D), has been extensively proven in vertical, horizontal and deviated wells. This process eliminates the conventional drill string by using the casing itself as the hydraulic conduit and means of transmitting mechanical energy to the drill bit. A short wireline-retrievable Bottom Hole Assembly (BHA) consisting of at least a drill bit and an expandable under-reamer are used to drill a hole of adequate size to allow the casing to pass freely.

DwC has been employed in many countries as an effective method of reducing the overall drilling costs by reducing drilling time and drill string problems encountered during conventional drilling process [2]. In addition to the productive drilling time

* Corresponding author at: YPF Tecnología S.A., Av. del Petróleo Arg. s/n, 1923 Berisso, Argentina.
E-mail address: pablo.g.cirimello@ypftecnologia.com (P.G. Cirimello).

http://dx.doi.org/10.1016/j.engfailanal.2016.11.008
1350-6307/

lost to tripping, unscheduled events during tripping can make the drilling process even more inefficient and even lead to losing the well. While the potential savings from reducing drill-string tripping and handling times are important, the savings from reducing hole problems may be more significant [3].

There are many situations where problems such as loss of circulation, well control incidents, and borehole stability problems are directly attributed to tripping the drill-string and other situations where these problems prevent the drill-string from being tripped. Since the CwD process provides a continuous ability to circulate the well, it is inherently safer than leaving the well static without a means of circulating it while a conventional drill-string is tripped. Reduced pipe tripping with CwD should also reduce surge and swab pressure fluctuations.

There are two basic methods of drilling with casing [4]:

1. a latched retrievable Bottom Hole Assembly (BHA) inside the casing that incorporates a mud-motor to drive a conventional bit and reamer
2. a surface system that rotates the hole casing, and a drillable "cement in place" drilling BHA. This drill bit is cemented and drilled out with the next drilling assembly.

DwC systems have been designed primarily for multi-well offshore platforms, multi-well operations on land, deep-water operations, and for situations requiring operators to drill through and place casing across problem formations quickly. This technology was applied successfully to drill through depleted zones showing wellbore instability problems and mud losses, as an alternative to underbalanced drilling.

However, casings have originally not been designed for this purpose and still, the pipes and connections are required to remain sealed in the well after sustaining a large amount of drilling cycles and possible damage [5]. This is particularly true in the case of rotating casings, and the parts that are prone to fatigue failures the threaded connections between individual tubes.

Casing drilling is one of the examples in which excessive torque and wear must be added to the casing design stage in order to obtain good well integrity. Fatigue is not an unknown failure mode for mechanical components, but it was considered as being un-important for well tubulars such as casing or tubing. With the advent of CwD, especially in deviated wells with small -radii deviations (or "doglegs"), rotating bending is the primary source for cyclic (mostly axial) tensile stresses in the casing walls.

Most recent casing connection evaluation test programs are based on ISO 13679 requirements [6], while, API RP 7G is the dominant testing program for drill stem applications [7]. With the evolution of casing drilling technology, connections are subjected to increasingly stringent well conditions. These conditions include higher pressures, higher temperatures, and higher mechanical loads for longer drilling periods. As a result, the performance of the connections under these conditions is of increasing concern.

Drilling with casing applications combine both, drilling and casing damage mechanisms. As a result, new test programs were required to adequately characterize connection performance when used in casing drilling applications [8].

Casing failure is among the foremost concerns associated with oil & gas drilling operations. The rate of casing failure, causing fluid or gas leakage, rises sharply as wells age [9]. Tubing-less hydraulic fracturing compounds the risk by exposing weakened areas of the casing to very high pressures that could create pathways to other formations causing potential environmental issues. As of yet, the risks associated with horizontal wells are unclear. Besides, 90% of casing failures occur at the connecting points that link each individual steel pipe together.

Based on the increased demand upon OCTG (Oil Country Tubular Goods) to serve the new technologies, many of the OCTG manufacturers are developing new systems in which the fatigue aspects are considered. The increase in non-typical uses of OCTG makes the design and selection criteria for these new applications more difficult than conventional well usage During the life of a well the fatigue load of a casing string may change from simple fatigue (high cycle) to low cycle fatigue.

Based on these changes, fatigue tests and damage accumulation calculations were applied in order to estimate and extend the total life of the casing. As high resistance to fatigue loading together with high overtorque and compression capacities are at the top of a list of required features for connections to be used in DwC techniques. Special connections with enhanced performance need to be developed. This led to the development and evaluation of "premium" connections for casing which were designed to stand cyclic loads and reach an extended number of cycles under such conditions. The development process of an integral connection for casing sizes targeting very demanding applications comprised Finite Element Analysis (FEA) and Full Scale Fatigue Test (FSFT) leading to Stress Concentration Factors (SCF) lower than 2 [10]. In addition, semi-premium connections are notably cheaper, and cover less demanding applications, with SCF lower than 3, good enough when low doglegs are present.

2. Drilling conditions of the failed casing

A cracked 9″ 5/8 diameter, # 40 lbs/ft, K55 casing failed during "drilling with casing" an oil well, when the drill bit reached a depth of 752 m, causing a costly string break. The threaded joints are API Buttress connections with internal shoulder. The failure analysis carried out includes physical and chemical material tests, and a numerical stress analysis at the T/C threaded joint when subjected to the operation loads, as actually logged during drilling.

Fig. 1a is an image of the failed casing at the broken section, on the side that was in the well and had to be fished. Fig. 1b is an image of the broken section, in the upper side. Fig. 2 shows a sketch of the threaded part of the casing, the circle indicates the

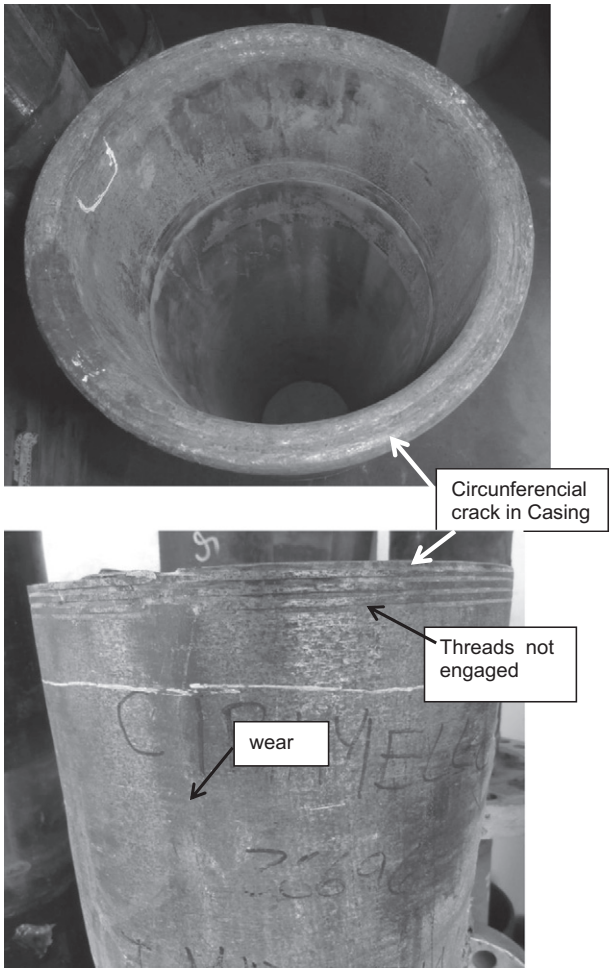

Fig. 1. Severed Casing: (a) upper part, (b) lower part ("fished").

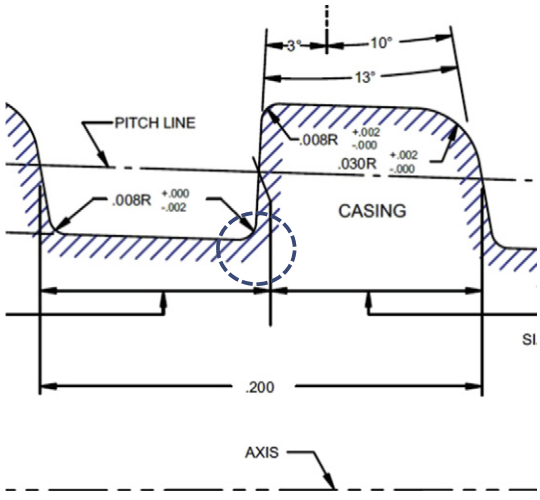

Fig. 2. Crack initiation site in Butress thread of failed casing.

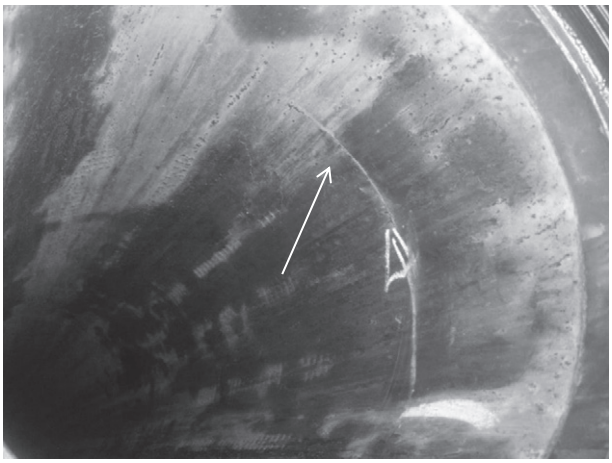

Fig. 3. Secondary crack in failed casing tube.

approximate position of crack initiation at the bottom of the thread. After fishing the casing string, two additional sections with cracks were found; one of them is shown in Fig. 3.

Relevant operating conditions for this failure event are:

- DwC was carried out using a 12″ dia. drill bit.
- Used drilling mud was water based bentonite.
- Pason logs allow having continuous records of torque, depth, rotation speed, weight on bit (WOB) and rate of penetration (ROP).
- Inclination and azimuth records are not available, so well tortuosity could not be assessed.
- After reaching a depth of 440 m, total fluid loss occurred, and drilling proceeded with no mud circulation.
- Particularly corrosive formations had not gone through.

Maximum recorded operating values are:

- Torque: 21,654 ft lb
- WOB: 31.4 Tn
- Rotation speed: 95 rpm (average speed 50 rpm)
- Hook load: 64.8 tons
- Surface pressure: 41 psi.

The analyses of the operating variables (Fig. 4) allow highlighting the following conditions:

- An increase in the torque range at 700–750 m depth; thus inferring the presence of vibrations transmitted by the casing.
- A noticeable decrease in ROP in the range of 725–750 m; a sign of difficulties in the performance of the drilling tool.

Both conditions are revealing some anomalous drilling conditions after reaching around 700 m.

3. Failure analysis

Brinell hardness values in tube and coupling materials [11] vary between 185 and 210 HB, typical of ferritic-pearlitic microstructures on C steel, showing no abnormalities in the analyzed areas. Table 1 shows the results of chemical analysis of tube material [12], and the limits required by the standard API 5 CT for a K55 grade [13]. Table 2 shows the results of tensile and impact testing from specimens taken near the failed region of the tube, [14] and API 5 CT limits for a K55 grade [13].

API 5 CT has no toughness requirements for this degree of casing. Longitudinal Charpy V notch 7.5 mm × 10 mm subsize specimens were machined from the wall of the failed casing, following ASTM A 370 [14]. The test was conducted according to ASTM E 23, at room temperature. Average absorbed energy is 30 J, which is equivalent to 40 J for standard specimens.

The chemical composition and mechanical properties of the failed casing comply with the requirements of API 5 CT K55. The casing material has a good toughness at service temperature.

Optical metallography of the casing material was conducted as per ASTM E 3 [15]. The specimens were 2% Nital etched. Fig. 5 (×100) shows a typical Pearlite - Ferrite microstructure. Note a rather coarse microstructure with heterogeneity in the size of pearlite colonies, and ferrite precipitated at grain boundaries, mainly related with a previous coarse austenite microstructure. Actual grain sizes range from 45 μm (fine grains) to 150 μm (coarse grains); grain size varies between 6 and 2–3 as defined by ASTM E112 [16].

Results of the visual inspection are:

1. The fracture surfaces are circumferential, normal to the tube wall

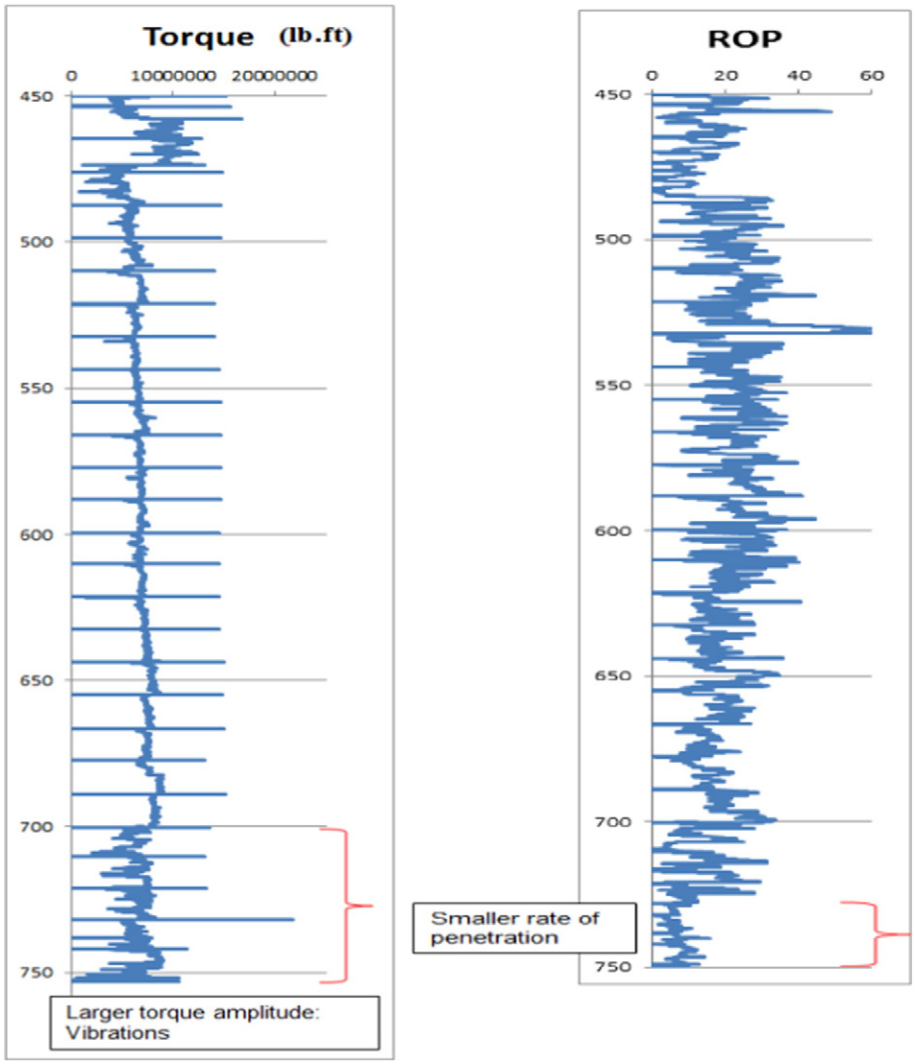

Fig. 4. Logs of (a) torque and (b) rate of penetration.

2. The fracture initiates in the outer (OD) wall surface of the tube (not in the coupling), at the position of the first engaged thread (Fig. 1).
3. The lower failed section was fished from the well, and shows typical damage produced by the fishing tool, with much of the failure evidence destroyed. Fig. 6 show indentations, loss of roundness and wear on the outer wall surface, all produced by the "crab type" fishing tool.

Table 1
Chemical compositions for *casing material.*

Element	Failed tube	API 5CT-K55
C	0.24	–
Mn	1.36	–
Mo	0.06	–
Cr	0.07	–
Ni	0.13	–
Cu	0.07	–
P	0.015	0.030 max
S	0.010	0.030 max
Si	0.35	–
V	0.002	–

Table 2
mechanical properties of failed *casing*.

Property	API 5CT – K55	Failed tube
Yield strength (MPa)	379–552	429
UTS (MPa)	655 min	698
Room temp. CVN (Joule)	–	40

4. Fracture surfaces have been plastically deformed by friction between faces after fracture (Fig. 1a), with an inhomogeneous layer of atmospheric corrosion.

Only the small portion shown in the insert of Fig. 7 was preserved from post-failure plastic deformation. As can be seen in the stereo microscopy and scanning electron microscopy (SEM) images of Fig. 7, this portion corresponds to micro void coalescence, related to the final ductile fracture.

The complete destruction of the evidence in the fracture surfaces created during in- service propagation could be overcome by the evidence obtained from a secondary crack found in the failed string, Fig. 3. This secondary crack is also circumferential and adjacent to the first engaged thread, i.e. analogous to the main fracture.

The SEM image of Fig. 8 shows ratchet and beach marks, typical of fatigue initiation of multiple micro-cracks from the bottom of the thread [17]. These multiple initiation sites are associated with high stress concentration, and are not associated to any metallurgical defect or unique discontinuity from manufacturing. No macroscopic plastic deformation was detected; no plastic indentations in the threads were found, that could indicate a possible excessive torque.

The SEM image in Fig. 9 shows a region in the surface of the secondary crack (Fig. 8) for which the crack depth is a = 20 mm. Fatigue striations are somewhat variable, an approximate average is 0.4 μm (5 striations in 2 μm, as seen in the picture).

From these fractographic analyses it can be concluded that the failure was due to fatigue crack nucleation and growth in the tube/coupling (T/C) transition zone, followed by ductile fracture due to tensile loads along the casing axis. No evidence of metallurgical defects associated with crack initiation was found.

4. Experimental fatigue evaluation

Fatigue is a mechanism associated with cyclic loading; 0.4 μm striations, as defined in Fig. 9, correspond to the steps in crack growth. These can be used as an in-situ indication of crack growth rate from which the applied crack driving forces could be inferred. However, how the striations relate to each loading cycle in ferritic pearlitic. Carbon steels is a matter of discussion [18]. To settle this, experimental fatigue tests were carried out to characterize initiation and propagation of fatigue cracks in base metal from the failed casing.

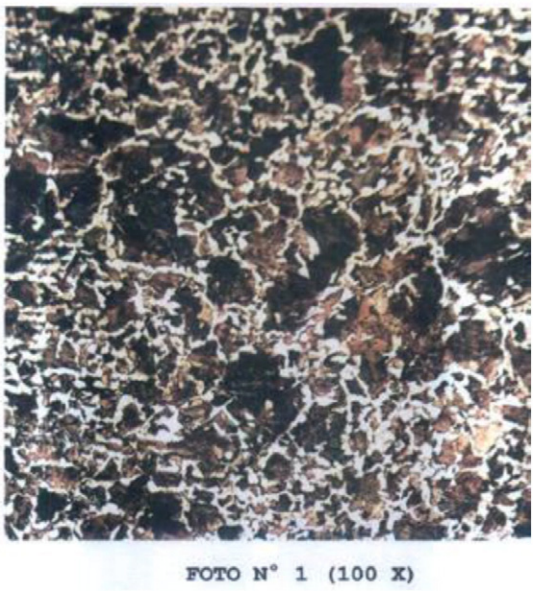

Fig. 5. Microstructure of *casing* material (100×).

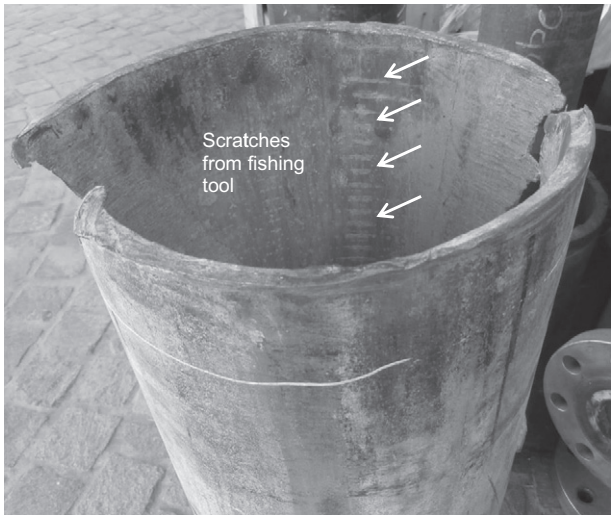

Fig. 6. Lower tract of failed casing.

Standard CT (compact tension) specimens were taken from the threaded end (Fig. A1.1, ASTM E647) [19]. Fatigue tests were performed using a 10 ton INSTRON 8801 machine. Instant crack length was measured during each test, using the so-called compliance method (ASTM E647, A1.5.2). Each test was carried out at constant load amplitude ($\Delta P = 6000$ N), with a load ratio $R = Pmin/Pmax = 0.1$. Fig. 10 shows the experimental relationship between crack propagation rates (da/dN) and the range of the applied stress intensity factor, ΔK. Note that these data fall into the so called Paris-Erdogan relationship between da/dN and the ΔK:

$$da/dN = C\Delta K^m$$

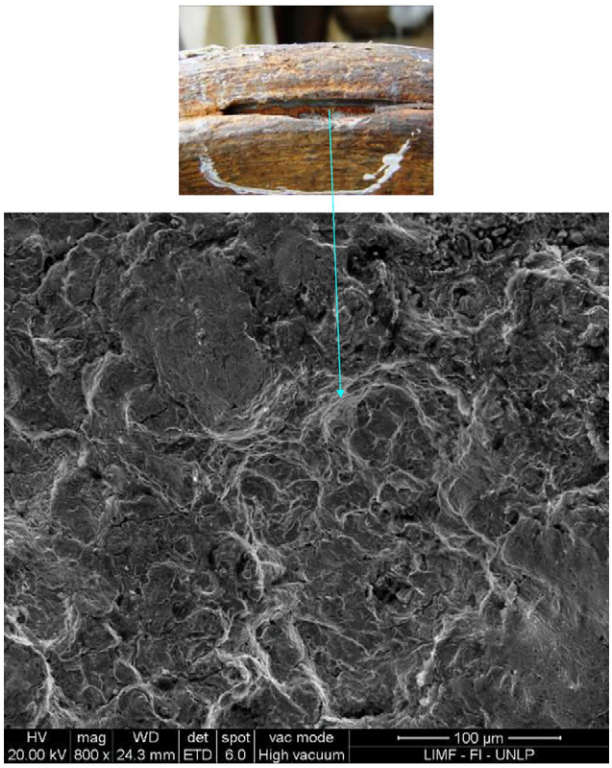

Fig. 7. ductile collapse in the single preserved portion of the main fracture.

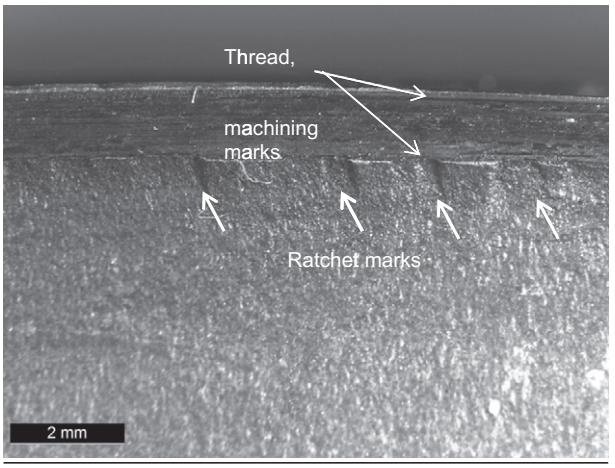

Fig. 8. Fracture surface of secondary crack in casing (Fig. 3).

Experimentally determined constants are: $C = 9\ E^{-10}$ mm/cycle, $m = 3.44$. The decreasing applied-ΔK methodology was used for measuring the fatigue crack growth threshold, ΔKo. Applied load was controlled according to the equation:

$$Cg = (1/K)\ (dK/da) = -0.06\ mm^{-1}$$

The absolute value for Cg was optimized according to specimen dimensions and load history, and is smaller than the maximum allowed ty the ASTM standard ($-0.08\ mm^{-1}$). Fig. 11 shows the da/dN vs. ΔK data points. The measured value for the propagation threshold is:

$$\Delta Ko = 8.8 \pm 0.5\ MPa\ m^{1/2}$$

SEM fractographic analysis allows the experimental verification of the correspondence between striation spacing and applied ΔK [20]. This was done in the lab specimens, in regions of the crack surfaces corresponding to three ΔK levels: $\Delta K \approx 35$, 55 and 65 MPa $m^{1/2}$ (defined by choosing the corresponding crack lengths). Fig. 12 shows fracture surfaces from each specimen, at different magnifications. Details show areas of crack growth by mechanisms of ductile cycle-to-cycle propagation, where corresponding striations are clearly identifiable.

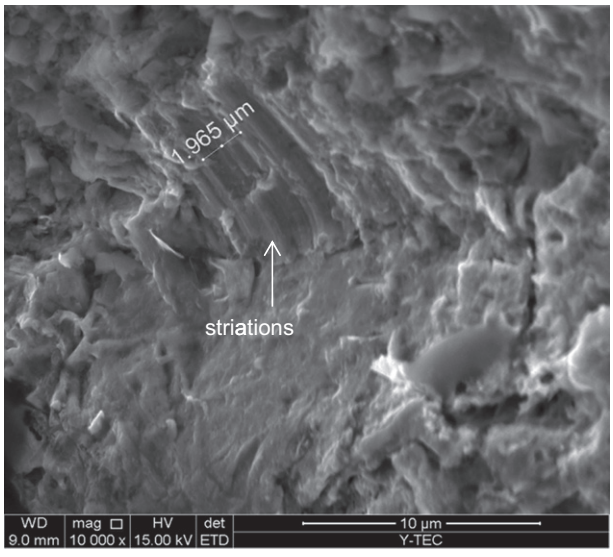

Fig. 9. Fatigue striations in secondary crack.

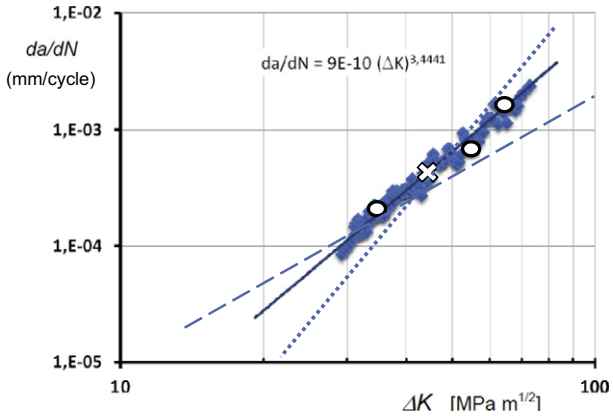

Fig. 10. Fatigue crack growth rate, da/dN vs. applied ΔK. Squares: from tests, circles: from Fig. 12, cross: from Fig. 8. Discontinuous lines from literature data.

Round symbols in Fig. 10 show the da/dN vs. ΔK data points obtained from this fractographic study. These observations are local; average growth rates, as measured macroscopically from load and displacement test measurements may be somewhat different. Nevertheless, these measurements of striation spacing allow defining a more than acceptable one-to-one correlation between each growth step and each stress cycle. In such case, it is possible to make a rough approximation of the ΔK actually applied to the secondary crack at the site seen in Fig. 3, Fig. 8 and Fig. 9. The cross symbol in Fig. 10 for a da/dN of 0.4 10^{-3} mm/cycle predicts a ΔK in the average of 45 MPa $m^{1/2}$.

5. Fracture mechanics model

The Finite Element Stress Analysis of the tube/coupling joint considers the operational conditions provided by the driller, and the geometrical characteristics of the joint, from open information by the manufacturer and API 5B [21] (Fig. 2). The following simplifications were made in the Abaqus linear elastic model [22]:

- The geometry of the Butress thread was considered as rectangular, while notch radii agree with those specified in API 5B, see Fig. 13(a).
- Symmetry: half the length of the couple was considered, and torque was applied to it.
- Coupling threads were considered perfect.
- To eliminate edge effects, around 2000 mm of casing tube was modelled and boundary conditions apllied at its end.

There are two levels of modeling:

- Level 1: conservative, assumes nominal depth of thread (1, 57 mm) at crack initiation
- Level 2: realistic, due to the cone-shaped thread, the depth of the thread that transfers the load between tube and coupling is around half nominal (0.8 mm)

The following operating conditions were considered:

- Maximum torque = 21654 ft lb = 29,358,882 Nmm
- Axial maximum load (maximum WOB, without torque) = 31.4 Tn = 307,929 N

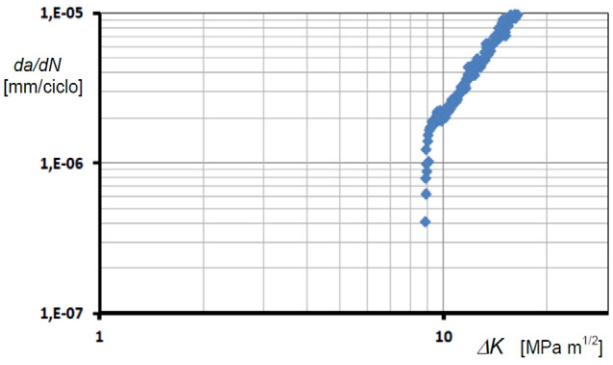

Fig. 11. da/dN vs. ΔK data points at near-threshold fatigue crack propagation.

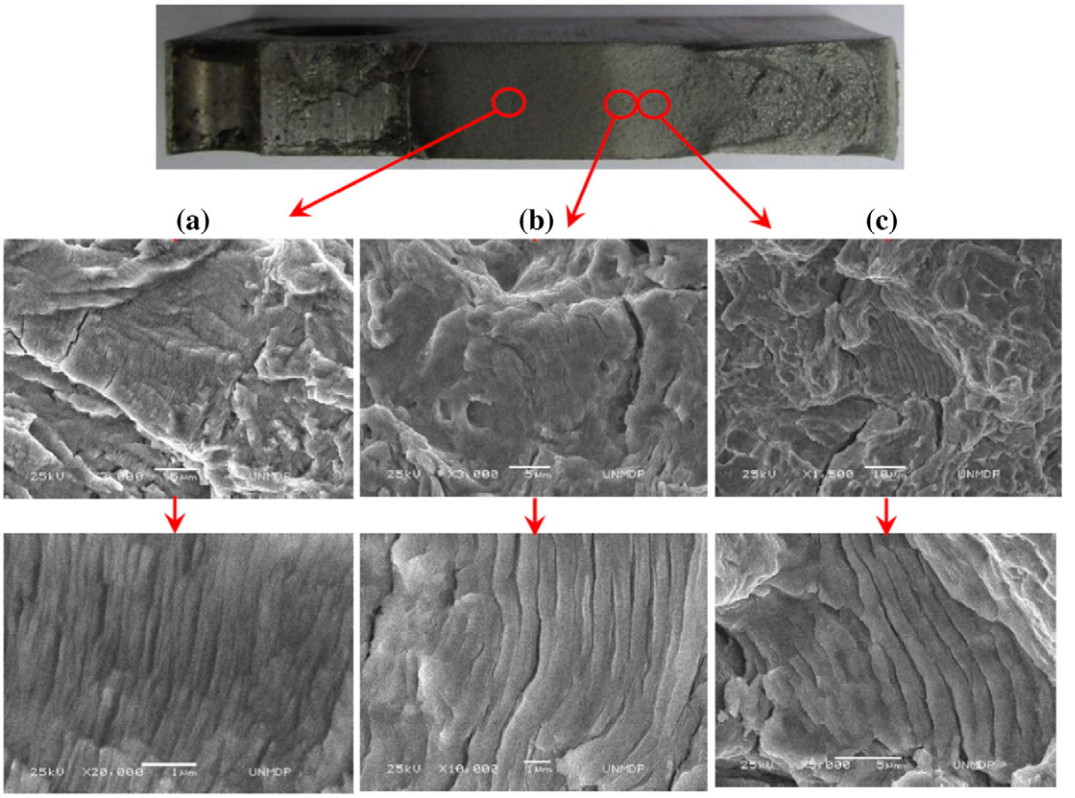

Fig. 12. Fracture surfaces at $\Delta K \approx$ (a) 35, (b) 55 and (c) 65 MPa $m^{1/2}$, details show ductile cycle to cycle propagation.

• Maximum combination of loads: torque = 10488 ft lb, axial load = 23.4 Tn = 229,476 N

Fig. 13(b) shows the resulting stress contour for the realistic model. As expected, the maximum stresses are found in the thread, where the T/C transition occurs, and where the failure occurred. It is seen that the maximum stress at the notch is 2.4 times greater than in the neighboring areas of the casing. This stress concentration factor (SCF) is within the range of expected SCF for threaded connections, see for instance [23] and casing manufacturer documentation [24].

Table 3 summarizes resulting stresses when considering (A) only operating torque and (B) only maximum compression, produced by the WOB. For the most critical combination of torque and compression: 10,488 ft lb torque and WOB = 23.4 tons, the respective Von Mises equivalent stresses are 125 MPa and 257 MPa respectively. The most severe condition predicts a combined maximum tensile stress in the area of the failed thread of 270 MPa. Therefore, the initiation of a fatigue crack occurred when the following condition was met:

$$\Delta K = Y\,\Delta\sigma\,(\pi\,a_i)^{1/2}$$

where a is the initial crack depth. Taking a shallow crack of little depth in the bottom of the notch, we can take Y = 1.12 [25]. For a threshold value $\Delta Ko = 9$ MPa $m^{1/2}$ and $\Delta\sigma = 270$ MPa, the minimum crack depth required to initiate the mechanism of fatigue

Table 3
results of the linear-elastic analysis at failed section for applied torque and compression.

Model	Torque ft lb	Compression Ton	σ_{VM} at notch MPa	σ_{VM} in casing MPa	σ_m failed section MPa	σ_b failed section MPa
Conservative	21,654		258,5	61,1	160	100
Realistic	21,654		238,0	61,1		
Conservative		31,4	344,8	41,6	190	150
Realistic		31,4	306,1	41,6		
Combined	21,654	31,4			160	110

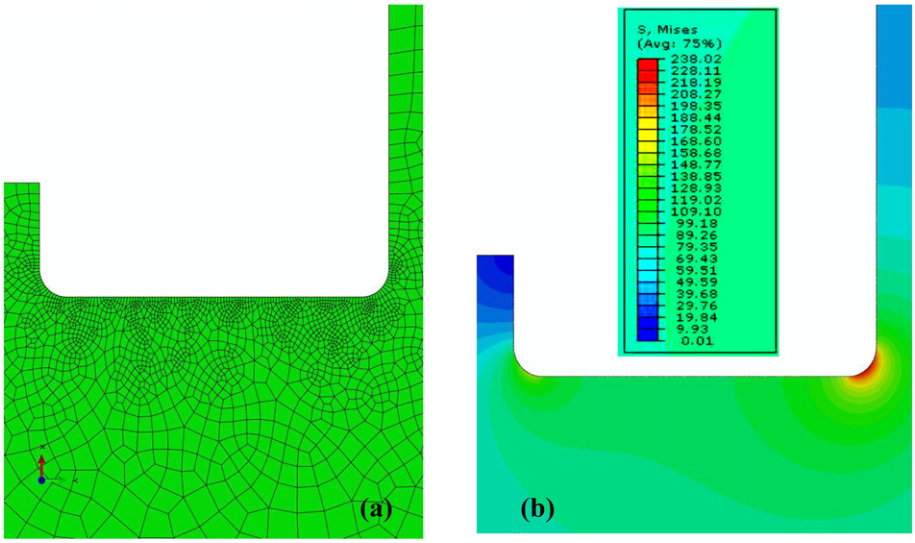

Fig. 13. FEM model. (a) mesh at root of first thread, as indicated in Fig. 2. (b) Von Mises Stress contour (MPa).

crack growth is

$$a_i = 0,30 \text{ mm}$$

In this case, service temperatures are well above the ductile-to-brittle transition of the tube material, so a close approximation to material fracture toughness can be obtained via the Rollfe-Novak-Barsom K_{IC}–CVN Upper Shelf Correlation [26]:

$$\left(\frac{K_{IC}}{\sigma_{ys}}\right) = 0.64\left(\frac{CVN}{\sigma_{ys}} - 0.01\right)$$

Here CVN is the full-size Charpy impact energy (J), σ_{ys} is the material yield strength (MPa), and K_{IC} is its fracture toughness in MPa $m^{1/2}$. So that:

$$K_{IC} = 105 \text{ MPa } m^{1/2}$$

The critical length (L_{crit}) of a circumferential through-the-thickness crack depends upon the distribution of equivalent membrane and bending stresses in the failed section, that is, the casing material outside the stress concentration in the thread. According to the stress analysis, at the time of final fracture (Table 3):

$$\sigma_m = 160 \text{ MPa}, \sigma_b = 110 \text{ MPa}$$

Since the applied stresses are much less than half the yield strength for the material, critical crack length can be determined via linear elastic fracture mechanics. Standard solutions for surface cracks in a plate subjected to membrane and bending stresses are expressed as [27]:

$$K_I = (\sigma_m + H\sigma_b)F\sqrt{\frac{\pi a}{Q}}$$

where Q is a shape parameter and F and H are geometric constants that depend on a/c (crack depth to length ratio), and a/t (crack depth to thickness ratio). Considering that the through-the-thickness crack developed at the failed section before final fracture was much shorter than the tube perimeter, the final fracture occurred when $K_I = K_{IC}$, $L_{crit} = 2a$, $Q = 1$, $F = 1$, $H = 0.66$. Therefore:

$$L_{crit} = 130 \text{ mm}$$

Tube perimeter is around 768 mm, so this model predicts that the fatigue crack had already spanned around 1/6th of the section when it became critical and final failure developed. The length of the secondary crack depicted in Fig. 6 is less than half the

predicted critical length. This is a further indication of the validity of these calculations for this crack would still have to grow to eventually lead to fracture.

Note that critical crack length for brittle fracture depends on the square of material toughness. Doubling material toughness would roughly change the condition of final failure to a fully plastic collapse, and critical crack length would be near half the casing perimeter. But this "advantage" represents only a small percentage in the total service life, since crack propagation would be quite fast in the final stages of fatigue growth. Fig. 10 predicts growth rates of 10^{-2} mm per cycle at $\Delta K = 100$ MPa $m^{1/2}$. So an extra 60 mm of crack growth at each crack tip (for an alleged critical length of 250 mm) would at the most require:

$$N = \Delta a/(da/dN) = 60/10^{-2} = 6000 \text{ rotation cycles}.$$

6. Discussion of results

Fractographic analyses identified fatigue crack nucleation and growth in the tube/coupling (T/C) transition zone. Fracture mechanics analyses allowed defining that the combination of operative torque and compression proved sufficient to reach material critical conditions in the T/C joint at the failure site. As a result, during drilling these joints are subjected to cyclic tensile stresses that can surpass the fatigue limit of the standard-grade casing under analysis.

The failed casing complies with all API 5CT standard requirements, in terms of chemical composition and mechanical properties, albeit a somehow heterogeneous metallographic microstructure that is far from those of steels having fine austenitic grains. API 5CT requirements for grade K55 do not include any mandatory heat treatments. Nevertheless, these casings can be normalized, normalized and tempered, or quenched and tempered, at the manufacturer's option or if specified by the buyer on the purchase order.

Experimental fatigue tests in tube material allowed defining material constants for crack growth (Paris equation, $C = 9$ E-10 mm/cycle, $m = 3.44$), that are within normal properties for a carbon steel; although a rather high fatigue threshold value ($\Delta Ko = 9$ MPa $m^{1/2}$) was obtained [28,29]. Experimentally determined fatigue growth rates in Fig. 10 are compared with

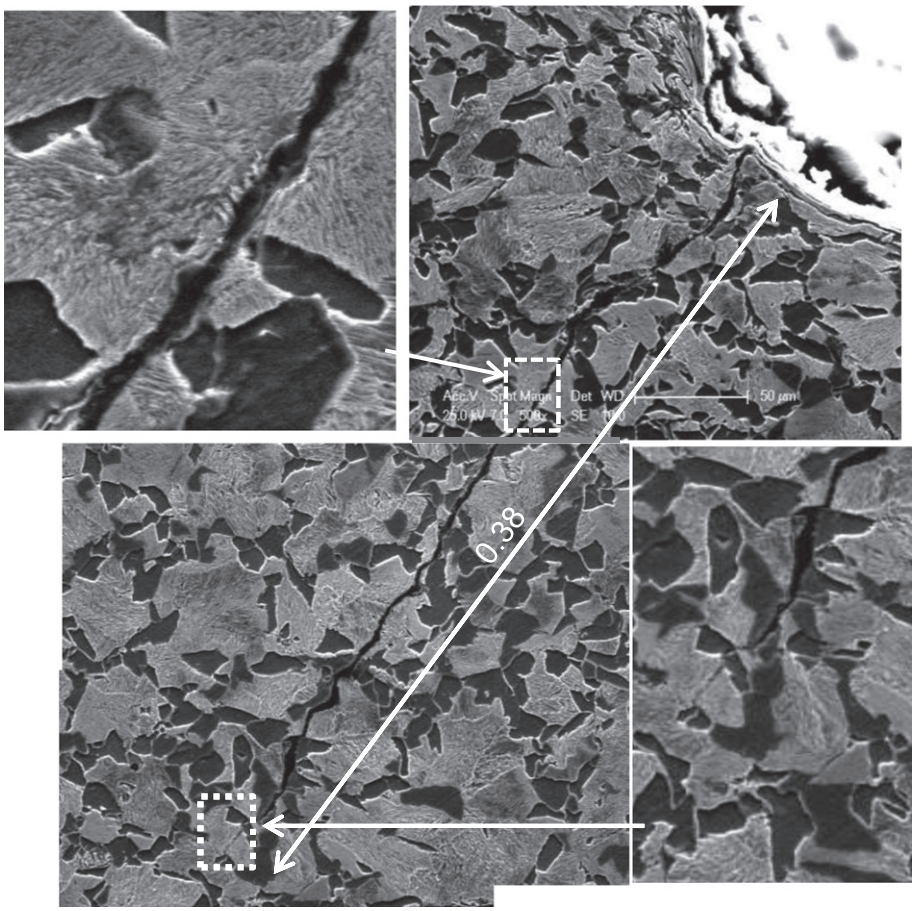

Fig. 14. Nital etched cross section of small crack in casing tube, initiated at bottom of thread (upper right). Note tortuous path along grains and grain boundaries.

experimental results for a ferritic pearlitic base material (dashed line) and welded tubulars (dotted line), as determined in [30,31]. Fatigue growth rates are within the upper limit of the expected range.

Considering the maximum cyclic stress $\Delta\sigma = 270$ MPa applied at the thread, the minimum crack depth required to initiate the mechanism of fatigue is

$$a_i = 0,30 \text{ mm}$$

The radius of curvature at the root of the thread is about 1 mm. A 0.3 mm deep defect is perfectly compatible with the zone influenced by the stress concentration at the thread. The stress analysis shows that combinations of torque and compression as those found in the operation records create a stress state in the T/C transition that justify fatigue crack initiation. The most critical operational condition in terms of combination of compression and torque gives rise to a stress state in the failed thread that leads to fatigue crack initiation from 0.3 mm deep defects.

This is compatible with non-propagating cracks that have been found in other samples of this same casing; see for instance the photographic composition of metallographic images in Fig. 14. This figure indicates how cracks could initiate at the bottom of the thread in the casing tube (upper right in the figure). Inserts show details of a rather tortuous path along grains and grain boundaries of the heterogeneous microstructure. Crack depth spans many grains ($a/M = 6.6 > 5$), so this crack could be defined as "microstructurally long". This crack is immersed in the stress concentration of the thread ($a/R = 1.2 < 4$), so it is "mechanically short" [32]. Note that the depth of the crack depicted is 0.38 mm, quite close to the 0.3 mm threshold depth previously defined for the applied stress conditions.

Most relevant is that future integrity of casings used for drilling could not be assured, unless the magnitudes of cyclic drilling stresses can be reduced below an allowable stress that must take into account the actual fatigue strength of tubes and connections. Fatigue cracks like those shown in this study would most likely be found in other pipes used for casing-drilling. These cracks, even though did not lead to fast fracture, would eventually lead to leaking during subsequent well production.

It is possible to envision a combination of geometric and material conditions that minimize the possibility of through-the-thickness cracks remaining in the tube wall after completing the drilling process. Chemical composition, heat treatment and improved joint efficiency are already available from OCTG manufacturers. But relying in costly, proprietary grades of casing tubes pretty much reduces the economic convenience for using the DwC procedure.

Better steels are often seen as fine grained, as grain refinement simultaneously leads to increased strength and toughness. But toughness is not the main controlling mechanical parameter in this case. Fatigue threshold is usually larger in coarse grained steels, since small fatigue cracks initiated within these large grains remain as "microstructurally short" for a longer time. This is the case in our steel, leading to reduced fatigue growth rates or even increasing the chances for cracks to stop growing and become non-propagating cracks.

The future integrity of casings used for drilling could be improved by reducing the probability of cracks initiated at the threaded joints that grow beyond 0.3 mm deep, but do not reach the fracture condition. A material with a combination of a large fatigue threshold and relatively low toughness, along with as small a stress concentration at threads as possible, would do the trick. For the case under study, therefore, there would be a need to improve the tube steel, but more important would be the benefit in switching to a better and more efficient, although more costly, more sophisticated threaded joint.

7. Conclusions

A recent failure, and at least two fatigue cracks found in the tube/coupling (T/C) transition zone of casings used for drilling oil and gas wells, arise doubts about integrity during the future service life of casings used for well drilling. Although the failed casing complies all API 5 CT standard requirements, DwC requires a string design that must consider resistance to fatigue (nucleation and initial crack growth), in order to avoid subcritical cracks that would later compromise well integrity.

To mitigate the occurrence of well failures during both, previous drilling and pursuing oil production, it is suggested to analyze the technical and economic feasibility of using more sophisticated tube-coupling designs. These would combine high toughness steels based on chemical composition and heat treatments, with improved connections. Large grained tube steels and premium connections seem best alternatives to ensure surviving cyclic torque and compression stresses without serious damage.

Acknowlegments

The authors thank YPF Tecnología S.A. for motivation and funding for this research and YPF S.A. for allowing the diffusion of proprietary information. Thanks are also given to funding by Conicet (Concejo Nacional de Investigaciones Cientificas y Tecnicas, Republica Argentina), and to Dr. Mirco Chapetti from Intema (Institute for Materials Science, Conicet) for experimental results and discussions.

References

[1] T. Warren, B. Houtchens, G. Madell, Directional drilling with casing, SPE Drilling ConferenceSociaety of Petroleum Engineers, The Netherlands, 2003.
[2] R.M. Tessari, T.M. Warren, Drilling with casing reduces cost and risk, SPE Russian Oil and Gas Technical ConferenceSociaety of Petroleum Engineers, Russia, 2006.
[3] Nediljka Gaurina-Međimurec Casing Drilling Technology. University of Zagreb, Croatia (ngaumed@rgn.hr)

[4] A. Fisher, D. Reid, M. Zo Tan, G. Galloway, Extending the boundaries of casing drilling, IADC/SPE 87998, SPE Asia Pacific Drilling Technology ConferenceSociaety of Petroleum Engineers, Malaysia, 2004.
[5] Q. Lu, D. Hannahs, Connection performance evaluation for casing-drilling applicationOTC 18495. Offshore Technology Conference, Houston, U.S.A, 2007.
[6] ISO 13679, Petroleum and Natural Gas Industries-Procedures for Testing Casing and Tubing Connections, first ed., 2002.
[7] API RP 7G, Recommended Practice for Drill Stem Design and Operating Limits, 16th ed., 2009 add. 1 & 2.
[8] C. Teodoriu, J. Schubert, Redefining the OCTG fatigue—A theoretical approachOTC 18458, Offshore Technology Conference, Houston, U.S.A., 2007.
[9] Hannah Wittmeyer, Well-casing-failure-violations, June 2013. http://frackwire.com.
[10] N.J. Santi, G.E. Carcagno, R. Toscano, Premium & semi-premium connections design optimization for varied drilling-with-casing applicationsOTC 17221, Offshore Technology Conference, Houston, U.S.A., 2005.
[11] ASTM E 384-11, Standard Test Method for Knoop and Vickers Hardness of Materials, ASTM International, 2011.
[12] ASTM E 415-14, Standard Test Method for Analysis of Carbon and Low Alloy Steel by Spark Atomic Emission Spectrometry, ASTM International, 2014.
[13] API 5CT, Specification for Casing and Tubing, API, 2012.
[14] ASTM A 370-13, Standard Test Methods and Definitions for Mechanical Testing of Steel Products, ASTM International, 2013.
[15] ASTM E3-11, Standard Guide for Preparation of Metallographic Specimens, 2011.
[16] ASTM E 112-13, Standard Test Methods for Determining Average Grain Size, ASTM International, 2013.
[17] ASM Handbook vol. 11, Failure Analysis and Prevention, ASM International, 1992.
[18] M.D. Chapetti, Report MEXCTI-14102015 Ensayos de propagación de fisuras por fatiga en acero, Medición de constantes de Paris y Umbral de propagación, Universtiy Mar del Plata, Argentina, 2015.
[19] American Society for Testing of Materials, ASTM E647, standard test method for measurement of fatigue crack growth rates, 1988.
[20] J.L. Otegui, M.D. Chapetti, J. Motylicki, Fatigue assessment of an E.R.W. oil pipeline, Int'l. Journal of Fatigue 24 (2002) 21–28 ISSN 0142-1123.
[21] API 5B, Specification for Threading, Gauging and Thread Inspection of Casing, Tubing and Line Pipe Threads, 2008.
[22] Abaqus/Standard®. User manual, Version 6.14. Dassault Systèmes.
[23] A.P. Boresi, R.J. Schmidt, Advanced Mechanics of Materials, 6th Ed Wiley, 2003.
[24] OTC 17221 - Premium & Semi-premium Connections Design Optimization for Varied Drilling-with-Casing Applications, Tenaris, 2015.
[25] T.L. Anderson, Fracture Mechanics: Fundamentals and Applications, second ed CRC Press, 1994.
[26] D.P. Miannay, Time-dependent Fracture Mechanics, Springer, Technology & Engineering, 2012 (ISBM 978-1-4612-6537-5).
[27] J.L. Otegui, Failure Analysis: Fundamentals and Applications in Mechanical Components, Springer, 2014.
[28] D. Radaj, C.M. Sonsino, D. Flade, Prediction of service fatigue strength of a welded tubular joint on the basis of local approaches, Int´l. Journal of Fatigue 20 (6) (1998) 471–480.
[29] S.W. Hong, J.M. Koo, C.S. Seok, J.H. Kim, S.K. Hong, Fatigue life prediction for an API 5L X42 natural gas pipeline, Eng. Failure Analysis 56 (2015) 396–402.
[30] J.L. Otegui, M.D. Chapetti, J. Motylicki, Fatigue assessment of an E.R.W. oil pipeline, Int'l. Journal of Fatigue 24 (2002) 21–28.
[31] P.G. Fazzini, J.C. Belmonte, M.D. Chapetti, J.L. Otegui, Fatigue Assessment of a Double Submerged Arc Welded Gas Pipeline, Int'l. Journal of Fatigue 29 (2007) 1115–1124.
[32] ASM Metals Handbook, Fatigue and Fracture, Vol.19, ASM International 1996, pp. 374–380.